



HAL
open science

Relativistic Quantum Field Theory Approach to Electron Wavepacket Tunneling: a Fully Causal Process

M Alkhateeb, X Gutierrez de la Cal, M Pons, D Sokolovski, A Matzkin

► **To cite this version:**

M Alkhateeb, X Gutierrez de la Cal, M Pons, D Sokolovski, A Matzkin. Relativistic Quantum Field Theory Approach to Electron Wavepacket Tunneling: a Fully Causal Process. 2025. hal-04895869

HAL Id: hal-04895869

<https://hal.science/hal-04895869v1>

Preprint submitted on 19 Jan 2025

HAL is a multi-disciplinary open access archive for the deposit and dissemination of scientific research documents, whether they are published or not. The documents may come from teaching and research institutions in France or abroad, or from public or private research centers.

L'archive ouverte pluridisciplinaire **HAL**, est destinée au dépôt et à la diffusion de documents scientifiques de niveau recherche, publiés ou non, émanant des établissements d'enseignement et de recherche français ou étrangers, des laboratoires publics ou privés.

Relativistic Quantum Field Theory Approach to Electron Wavepacket Tunneling: a Fully Causal Process

M. Alkhateeb,¹ X. Gutierrez de la Cal,^{2,3} M. Pons,^{3,4} D. Sokolovski,^{2,3,5} and A. Matzkin⁶

¹*Research Unit Lasers and Spectroscopies (UR-LLS),
naXys & NISM, University of Namur,*

Rue de Bruxelles 61, B-5000 Namur, Belgium

²*Departamento de Química-Física, Universidad
del País Vasco, UPV/EHU, 48940 Leioa, Spain*

³*EHU Quantum Center, Universidad del País Vasco, UPV/EHU, 48940 Leioa, Spain*

⁴*Departamento de Física Aplicada, Universidad
del País Vasco, UPV/EHU, 48013 Bilbao, Spain*

⁵*IKERBASQUE, Basque Foundation for Science, E-48011 Bilbao, Spain*

⁶*Laboratoire de Physique Théorique et Modélisation,
CNRS Unité 8089, CY Cergy Paris Université,
95302 Cergy-Pontoise cedex, France*

Abstract

Recent results on electron tunneling across a potential barrier, inferred from observations or obtained from theoretical models, have suggested superluminal or instantaneous barrier traversal times. In this work we investigate relativistic wavepacket dynamics for an electron tunneling through a potential barrier employing space-time resolved solutions to relativistic quantum field theory (QFT) equations. We prove by linking the QFT property of microcausality to the wavepacket behavior that the tunneling dynamics is fully causal, precluding instantaneous or superluminal effects. We illustrate these results by performing numerical computations for an electron tunneling through a potential barrier for standard tunneling as well for Klein tunneling. In all cases (Klein tunneling or regular tunneling across a standard or a supercritical potential) the transmitted wavepacket remains in the causal envelope of the propagator, even when its average position lies ahead of the average position of the corresponding freely propagated wavepacket.

I. INTRODUCTION

Tunneling is one of the most intriguing quantum phenomena. Although tunneling underlies many important processes in about every area concerned by quantum physics (see e.g. [1–7] for recent observations), its precise mechanism has remained controversial [8, 9]. Despite experimental data coming from different areas, from strong field tunneling ionization [2, 5, 10–12] to cold atoms [3] neutron optics [13] or condensed matter [14], there seems to be no solution in view [15] to the tunneling time problem (the time spent by a particle inside the barrier), or equivalently the arrival time (whether a particle that tunnels through a barrier arrives earlier than a freely propagating particle). Indeed, due to the ambiguity of measuring time in quantum mechanics – there is no time operator in the standard formalism – any observed tunneling time will depend on the model employed to extract the time interval from the observed data.

In particular, experiments involving electron photoionization have reported results interpreted to indicate instantaneous tunneling times [2, 5, 10, 11]. Such interpretations rely on models that intrinsically involve disputed approximations [16], generally employing a non-relativistic and often semiclassical framework. Perhaps somewhat more surprisingly, several works based on a first-quantized relativistic framework [17–25] have concluded on the possibility of superluminal arrival times for electrons. Such superluminal transmissions could potentially bring serious issues with causality, even though it is sometimes asserted that these effects do not seem to lead to signaling [24]. Other investigations carried out within relativistic quantum mechanics have on the contrary not noted any superluminal effects at the level of the wavefunction [26–29].

In this work, we investigate the tunneling dynamics in a second quantized framework. More specifically, we will employ a computational relativistic quantum field theory (QFT) approach in order to follow the space-time resolved dynamics of an electron tunneling through an electrostatic potential barrier represented by a background field. The electron is modeled as a wave-packet initially defined on a compact support launched towards a potential barrier. We will prove that microcausality of the fermionic quantum field implies that the electron wavepacket density evolves causally, thereby ensuring the absence of any superluminal effects such as instantaneous tunneling times. The present method allows us to treat on the same footing different types of tunneling effects: the familiar one charac-

terized by exponentially decaying waves inside the barrier, as well as Klein tunneling (with undamped oscillating waves in the barrier) for supercritical barriers (that is barriers with a potential above the pair-production threshold).

We will begin by describing our theoretical approach in Sec. II, where we will define the wavepacket as a second quantized state and introduce the particle density operator from field operators obeying the Dirac equation. In Sec. III, we will see that microcausality holds for a fermionic field in the presence of a background potential and use this result to show that the tunneled wavepacket density is constrained by a causal evolution – the wavepacket density cannot leak outside the light-cone. We will then give (Sec. IV) numerical results obtained with our QFT framework for three typical cases of tunneling, all cases displaying a causal behavior of the transmitted wavepacket: standard tunneling through a non-radiating barrier (similar to the familiar tunneling situation known in non-relativistic quantum mechanics), standard tunneling in the presence of a slightly radiating barrier (in which the transmitted wavepacket is overshadowed by the electron density due to pair-production), and Klein tunneling through a supercritical barrier, in which it is known that tunneling is mediated by pair production. We will discuss our results and conclude in Sec. V.

II. FRAMEWORK: QFT WITH A BACKGROUND POTENTIAL

A. First and second quantized evolutions

Our approach is based on a computational QFT framework [30], recently extended to treat particle scattering across a finite barrier [31] (see also [32, 33] for related recent work). In this framework, an electron wavepacket is described by a relativistic fermionic Dirac field, while the potential barrier on which the electron scatters will be described by a background “classical” field [34].

Let us first introduce the free Dirac Hamiltonian

$$H_0 = -i\hbar c \alpha_x \partial_x + \beta m c^2 \tag{1}$$

which has the eigenvalues $\pm |E_p| = \pm \sqrt{p^2 c^2 + m^2 c^4}$. α and β are the usual Dirac matrices (recall that in one spatial dimension, we can neglect spin-flip and replace α_x and β by the Pauli matrices σ_1 and σ_3 respectively), m the electron mass and c is the light velocity. The

positive and negative energy solutions of Eq. (1) are respectively given by

$$\begin{aligned} v_p(x) &= \begin{pmatrix} 1 \\ \frac{cp}{mc^2 + E_p} \end{pmatrix} e^{ipx} \\ w_p(x) &= \begin{pmatrix} 1 \\ \frac{cp}{mc^2 - E_p} \end{pmatrix} e^{-ipx} \end{aligned} \quad (2)$$

The full first quantized Hamiltonian

$$H = H_0 + V(x) \quad (3)$$

where $V(x)$ is a rectangular-like potential barrier. The Hamiltonian H generates a unitary evolution. Let U denote the unitary evolution operator of the full Hamiltonian with elements in the free Dirac basis given by

$$U_{v_k w_p}(t) \equiv \langle v_k | \exp(-iHt/\hbar) | w_p \rangle. \quad (4)$$

The second quantized creation and annihilation operators for particle and antiparticles will be labeled b_p^\dagger and b_p (for particles) and d_p^\dagger and d_p (for antiparticles). Since we are dealing with a fermionic field the creation and annihilation operators anti-commute, $[b_p, b_k^\dagger]_+ = [d_p, d_k^\dagger]_+ = \delta(p-k)$. $|0\rangle$ defines the vacuum state, i.e. $b_p|0\rangle = d_p|0\rangle = 0$. We will be working as usual in the Heisenberg picture, so that these operators evolve according to [30]

$$b_p(t) = \int dk (U_{v_p v_k}(t) b_k(0) + U_{v_p w_k}(t) d_k^\dagger(0)) \quad (5)$$

$$d_p^\dagger(t) = \int dk (U_{w_p v_k}(t) b_k(0) + U_{w_p w_k}(t) d_k^\dagger(0)) \quad (6)$$

and their conjugates. Eqs. (5) and (6) give the QFT dynamics in terms of the first quantized evolution operators. These equations will be seen to be the building blocks of to carry out numerical computations.

B. Densities and field operators

For the purpose of investigating causality, we find it convenient for a matter of presentation to start from an initial wavepacket perfectly localized within a compact spatial support. The second quantized state describing this initial wavepacket is written as

$$|\chi\rangle = \int dp (g_+(p) b_p^\dagger(0) + g_-(p) d_p^\dagger(0)) |0\rangle, \quad (7)$$

where $g_{\pm}(p)$ are the wavepacket amplitudes in momentum space. As it is well-known [35, 36] a compactly localized state must contain both positive and negative energy components, hence the presence of both creation operators b_p^\dagger and d_p^\dagger in Eq. (7).

The particle density at any given time is given by the expectation value

$$\rho(t, x) = \langle\langle \chi | \hat{\rho}(t, x) | \chi \rangle\rangle \quad (8)$$

where the density operator $\hat{\rho}(t, x)$ is defined by

$$\hat{\rho}(t, x) = \hat{\Phi}^\dagger(t, x) \hat{\Phi}(t, x). \quad (9)$$

Recall that in the absence of a wavepacket, the density would be given instead by the vacuum expectation value $\langle\langle 0 | \hat{\rho}(t, x) | 0 \rangle\rangle$.

$\hat{\Phi}(t, x)$ is the field operator. Since we are working with states having compact spatial support, we depart from the usual definition of the field operators and define them instead through [37]

$$\hat{\Phi}(t, x) = \int dp (\hat{b}_p(t) v_p(x) + \hat{d}_p(t) w_p(x)) \quad (10)$$

and its Hermitian conjugate

$$\hat{\Phi}^\dagger(t, x) = \int dp (\hat{b}_p^\dagger(t) v_p^\dagger(x) + \hat{d}_p^\dagger(t) w_p^\dagger(x)). \quad (11)$$

Indeed the standard field operators [36] cannot describe a compactly localized state. We stress however that the results described in this work do not depend on taking an initial compact state – the proofs given below also hold for the standard field operators and the quantum states of pure positive energy presenting infinite tails. The field operators (10)-(11) obey an important property: the equal-time anti-commutator is given by

$$[\hat{\Phi}^\dagger(t, x'), \hat{\Phi}(t, x)]_+ = \delta(x' - x) \quad (12)$$

just like the familiar field operators of the free Dirac field [38]. Eq. (12) is proved in Appendix A.

The computation of the density proceeds by plugging-in Eqs. (9), (7) and (10)-(11) into

Eq. (8). This gives

$$\rho(t, x) = \langle\langle 0 | \int dp (g_+^*(p) \hat{b}_p + g_-^*(p) \hat{d}_p) \quad (13)$$

$$\left\{ \iint dp_1 dp_2 v_{p_1}^\dagger(x) v_{p_2}(x) \hat{b}_{p_1}^\dagger(t) \hat{b}_{p_2}(t) \quad (14)$$

$$+ \iint dp_1 dp_2 w_{p_1}^\dagger(x) w_{p_2}(x) \hat{d}_{p_1}^\dagger(t) \hat{d}_{p_2}(t) + \quad (15)$$

$$\left(\iint dp_1 dp_2 v_{p_1}^\dagger(x) w_{p_2}(x) \hat{b}_p^\dagger(t) \hat{d}_p(t) + HC \right) \} \quad (16)$$

$$\int dp (g_+(p) \hat{b}_p^\dagger + g_-(p) \hat{d}_p^\dagger) |0\rangle\rangle, \quad (17)$$

where HC is the conjugate of the preceding term. This density can be parsed as a sum of three terms, each term corresponding to the expectation value obtained for each of the lines given by Eqs. (14)-(16),

$$\rho(t, x) = \rho_1(t, x) + \rho_2(t, x) + \rho_3(t, x). \quad (18)$$

$\rho_1(t, x)$ represents a “particle” density, in the sense in which ρ_1 is given only in terms of the positive energy spinor v_p of Eq. (2). The computation is derived by following Eqs. (B1)-(B5) of Appendix B. For the same reason, $\rho_2(t, x)$ will be said to represent an “antiparticle” density [it is given by Eq. (B6)], and $\rho_3(t, x)$ represents a “mixed term” [see Eq. (B7)].

Note while ρ_3 only depends on the wavepacket (ρ_3 vanishes if there is no wavepacket), in the expressions of ρ_1 and ρ_2 there is only a single term that does not depend on the wavepacket (the first line in Eqs. (B5) and (B6)). This term gives the density originating from pair production. Hence by subsuming these two lines into $\rho_{vac}(t, x)$, the total density can also be parsed as

$$\rho(t, x) = \rho_{vac}(t, x) + \rho_{wp}(t, x), \quad (19)$$

where ρ_{vac} is the “vacuum” particle density (due solely to the background potential) and ρ_{wp} is the part of the density due to the presence of the wavepacket.

The total number of particles $N(t) = \int dx \rho(t, x)$, obtained by integrating the density over all space, can be parsed as [37]

$$N(t) = \int dx (\rho_1(t, x) + \rho_2(t, x)) = N_{vac}(t) + 1 \quad (20)$$

given that $\int dx \rho_3(x) = 0$ (the wavepacket counts as one particle). $N(t)$ can also be written as the normal-ordered expectation value of the number operator $\hat{N}(t)$ written in the standard form

$$\hat{N}(t) = \int dp (\hat{b}_p^\dagger(t) \hat{b}_p(t) + \hat{d}_p^\dagger(t) \hat{d}_p(t)). \quad (21)$$

III. MICROCAUSALITY AND THE IMPOSSIBILITY OF SUPERLUMINAL TUNNELING

A. Microcausality with a background field

Microcausality as a general statement is the assertion that observables that are space-like separated commute. While it may sometimes be considered as an axiom in some versions of QFT [39], microcausality can be explicitly proved for some given quantum fields. In particular the proof that a non-interacting free Dirac field obeys microcausality is a well-known textbook result [38, 40]: if $\hat{O}(t, x)$ and $\hat{O}'(t', x')$ are two observables then

$$[\hat{O}'(t', x'), \hat{O}(t, x)] = 0 \quad (22)$$

for $c^2(t' - t)^2 - (x' - x)^2 < 0$. The standard proof involves writing an arbitrary observable as a bilinear combination of field operators,

$$\hat{O}(t, x) = \hat{\Phi}^\dagger(t, x) o(t, x) \hat{\Phi}(t, x) \quad (23)$$

where $o(t, x)$ is a matrix consisting of c -numbers [38, 40]. The commutator in Eq. (22) is then written in terms of the anti-commutators $[\hat{\Phi}^\dagger(t', x'), \hat{\Phi}(t, x)]_+$. For free Dirac fields, these anti-commutators can be computed in closed form [38] and are proved to vanish for space-like separated intervals. Note that the density operator given by Eq. (9) is the simplest bilinear form involving field operators; this is the only observable we will be interested in in this work.

A straightforward way to verify that microcausality holds here for free Dirac fields is to compute the commutator (22) in a reference frame in which the events are simultaneous, which is always possible (due to Lorentz invariance) for space-like separated points. In this reference frame the commutator for the density becomes $[\hat{\rho}(t, x), \hat{\rho}(t, y)]$ (with $x \neq y$) which can be readily computed as

$$\begin{aligned} [\hat{\rho}(t, x), \hat{\rho}(t, y)] &= \hat{\Phi}^\dagger(t, x) \left([\hat{\Phi}(t, x), \hat{\Phi}^\dagger(t, y)] \hat{\Phi}(t, y) + \hat{\Phi}^\dagger(t, y) [\hat{\Phi}(t, x), \hat{\Phi}(t, y)] \right) \\ &\quad + \left([\hat{\Phi}^\dagger(t, x), \hat{\Phi}^\dagger(t, y)] \hat{\Phi}(t, y) + \hat{\Phi}^\dagger(t, y) [\hat{\Phi}^\dagger(t, x), \hat{\Phi}(t, y)] \right) \hat{\Phi}(t, x) \\ &= \hat{\Phi}^\dagger(t, x) [\hat{\Phi}(t, x), \hat{\Phi}^\dagger(t, y)]_+ \hat{\Phi}(t, y) - \hat{\Phi}^\dagger(t, y) [\hat{\Phi}^\dagger(t, x), \hat{\Phi}(t, y)]_+ \hat{\Phi}(t, x) \\ &= 0 \quad (x \neq y) \end{aligned} \quad (24)$$

where the last line follows from Eq. (12) involving the equal time field anti-commutators.

It turns out that Eq. (12) also holds for non-interacting Dirac fields in the presence of a background potential. The proof is given in Appendix A (see Eqs. (A5)-(A9)). Therefore Eq. (24), the microcausality condition for the density observable, also holds in the presence of a potential barrier. We now hinge on this result to show that the density resulting from tunneling cannot display a superluminal behavior.

B. Microcausality and wavepacket tunneling

We consider the following situation. An electron wavepacket is prepared, say to the left of a potential barrier, with its density initially ($t = 0$) localized within a compact support \mathcal{D} defined by $\mathcal{D} = [x_-, x_+]$. Let us label x_0 to be the position of the wavepacket maximum at $t = 0$, and x_+ being the point closest to the barrier. The wavepacket is launched towards the barrier; we are interested in the part of the electron density due to the wavepacket's dynamical evolution appearing to the right of the barrier density, i.e. the part that has tunneled through the barrier.

Let x' be a point located to the right of the barrier and $\rho(t', x')$ the density at that point. This density is given as per Eq. (8) by the expectation value

$$\rho_\chi(t', x') = \langle\langle \chi \| \hat{\rho}(t', x') \| \chi \rangle\rangle. \quad (25)$$

To be clear ρ_χ represents the full electron density at (t', x') when an initial wavepacket is present; the origin of this density can either be due to the wavepacket or to the electron/positron pairs created by the potential. Let us now write the density at (t', x') in a different setting, identical to the preceding one except that there is no wavepacket at $t = 0$. This density is now given by the vacuum expectation value

$$\rho_0(t', x') = \langle\langle 0 \| \hat{\rho}(t', x') \| 0 \rangle\rangle, \quad (26)$$

and a non-vanishing density can only result from the pair production process.

Assume (t', x') and $(t = 0, x_+)$ are space-like separated, implying that (t', x') is space-like separated from any point of \mathcal{D} over which the wavepacket is non-zero at $t = 0$. Let us define the function

$$\mathcal{C}(t', x'; 0, x) = \langle\langle \chi \| \hat{\rho}(t', x') \hat{\rho}(0, x) \| \chi \rangle\rangle, \quad x \in \mathcal{D} \quad (27)$$

correlating an observation of the density at a position x inside the initial wavepacket followed by an observation of the density at the space-like separated point (t', x') . From Eqs. (7) and (10) we obtain, using $\hat{b}_p \hat{b}_{p'}^\dagger |0\rangle = \delta(p - p') |0\rangle$ and $\hat{d}_p \hat{d}_{p'}^\dagger |0\rangle = \delta(p - p') |0\rangle$,

$$\hat{\Phi}(0, x) \|\chi\rangle = \int dp (g_+(p)v_p(x) + g_-(p)w_p(x)) |0\rangle = \chi(0, x) |0\rangle. \quad (28)$$

Similarly we have

$$\langle\langle \chi | \hat{\Phi}^\dagger(0, x) = \langle\langle 0 | \chi^\dagger(0, x). \quad (29)$$

We can now write Eq. (27) as

$$\mathcal{C}(t', x'; 0, x) = \langle\langle \chi | \hat{\rho}(t', x') \hat{\rho}(0, x) | \chi \rangle\rangle = \rho_0(t', x') \rho_\chi(0, x), \quad x \in \mathcal{D} \quad (30)$$

where we have used the definition (9), Eqs. (28)-(29) and the fact that both $\hat{\Phi}^\dagger(t', x')$ and $\hat{\Phi}(t', x')$ anti-commute with $\hat{\Phi}(0, x)$ given that the two spacetime points $(0, x)$ and (t', x') are space-like. We have also used Eqs. (25)-(26), writing

$$\rho_\chi(0, x) = \langle\langle \chi | \hat{\rho}(0, x) | \chi \rangle\rangle = \chi^\dagger(0, x) \chi(0, x). \quad (31)$$

Eq. (30) implies not only that the densities at the two space-like separated points are independent, but further highlights that the density at (t', x') is a *vacuum* expectation value – that is it does not depend at all on the wavepacket (it can nevertheless be non-zero due to pair-production induced by the potential). Eq. (30) rules out the possibility of superluminal tunneling, because in that case there would be some space-time points (t', x') outside the light-cone for which the density at that point would depend on the presence and shape of the wavepacket. It is noteworthy that the result (31) does not depend on the shape, width or height of the background potential. This result holds of course for all types of tunneling – for regular tunneling (characterized by an exponentially decreasing density inside the barrier) or for Klein tunneling (oscillating particle density inside the barrier).

IV. ILLUSTRATIONS

A. Method

We illustrate here our QFT approach by carrying out numerical computations for an electron wavepacket, initially localized on a compact support, launched towards a background

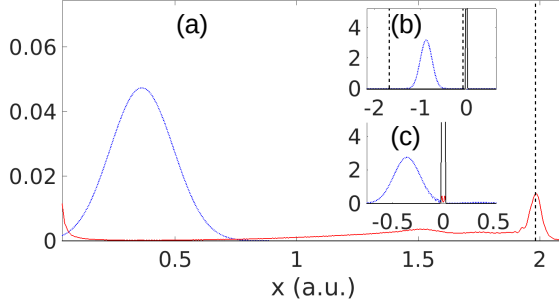


Figure 1. Space-time resolved densities for the Case 1 tunneling wavepacket. (a) The density of the transmitted wavepacket is shown (dotted blue) as it is exiting the barrier ($t = 1.5 \times 10^{-2}$ a.u.) for a comparatively low potential ($V_0 = 0.5mc^2$) giving rise to standard tunneling, with a negligible pair creation rate (the electron density created by the potential is shown in red). The inset displays snapshots of the wavepacket dynamics at (b) $t = 0$ and at (c) $t = 1.5 \times 10^{-2}$ a.u. (note the transmitted wavepacket is hardly visible on that scale in (c)). The dotted vertical line in (b) represents the right edge of the support \mathcal{D} over which the initial wavepacket is defined. The same line in (a) and (c) represents the position of the light-cone emanating from this right edge at the time of the plot. The initial wavepacket parameters in atomic units (a.u.) are $x_0 = -120\lambda$, $p_0 = 100$ a.u. and $\mathcal{D} = 70\lambda$ and for the barrier $L = 4\lambda$ and $\varepsilon = 0.3\lambda$, where $\lambda = \hbar/mc$ is the Compton wavelength of the electron.

potential having a rectangular-like shape. We will focus on the transmitted part of the wavepacket and consider 3 typical cases encompassing both standard and Klein tunneling. In the first illustration, we will consider a “low” background potential displaying features similar to the familiar non-relativistic tunneling case, characterized by a wavepacket mostly reflected and transmitted with a very small amplitude. In the second illustration, we will increase the potential barrier, which remains below the supercritical threshold ($2mc^2$) but is already sufficient in order to visualize the non-trivial interplay between the transmitted wavepacket and the exponentially small electron density due to pair production. In the third illustration, we will consider a background potential lying in the supercritical regime, with a wavepacket energy giving rise to Klein tunneling: the density oscillates inside the barrier and the wavepacket is transmitted with a very high amplitude.

To be specific, we will deal in all cases with an initial wave-packet given by the Dirac spinor

$$G(x) = \left(\cos^8\left(\frac{x-x_0}{D}\right)e^{ip_0x}, 0 \right) [\theta(x-x_-) - \theta(x-x_+)] \quad (32)$$

defined to be non-zero only over the compact support $x \in \mathcal{D}$ (θ is the units-step function). \mathcal{D} is defined by $\mathcal{D} = [x_-, x_+]$ with $x_{\pm} = x_0 \pm D\pi/2$ and is localized to the left of the barrier (πD is the length of the support and x_0 is the position of the maximum of the wavepacket). The \cos^8 function was chosen for computational convenience; p_0 is the initial mean momentum. p_0 and D are chosen such that the electron wavepacket moves towards the right as time evolves and the entire wavepacket remains below the potential threshold. By projecting $G(x)$ over the free Dirac basis $v_p(x)$ and $w_p(x)$ we obtain the coefficients $g_{\pm}(p)$ of Eq. (7) defining the initial second quantized wave-packet¹ which is in turn fed in Eq. (8) in order to obtain the space-time resolved density $\rho(t, x)$.

To this end we need to compute the unitary evolution elements appearing in the density expressions [see Eqs. (B5)-(B7)], such as $U_{v_k w_p}(t)$ given by Eq. (4). The background potential is set to be

$$V(x) = \frac{V_0}{2} [\tanh((x + L/2)/\epsilon) - \tanh((x - L/2)/\epsilon)] \quad (33)$$

where V_0 and L are the barrier height and width respectively and ϵ a smoothness parameter. We then determine the evolution operator by solving the corresponding Dirac equation on a discretized space-time grid using a split operator [42] method (the evolution operator is split into a kinetic part propagated in momentum space and a potential-dependent part solved in position space). Note that in order to simplify the numerics we have chosen $t = 0$ as the time the barrier is raised and starts radiating and also as the time the wavepacket is launched (although these two starting times are independent).

B. Standard tunneling

1. Case 1

Fig. 1 shows the transmitted wavepacket as well as the electron density due to pair production for a comparatively “low” potential ($V_0 = 0.5mc^2$). Snapshots of the density evolution are given in the inset; leaving aside pair production, this situation is a QFT account of the familiar Schrödinger-type tunneling dynamics, where most of the incoming electron amplitude is reflected and only a very small amplitude is transmitted.

¹ Recall that the first quantized wavepacket is obtained from the Fock space state through $\chi(t, x) = \langle\langle 0 | \hat{\Phi}(t, x) | \chi \rangle\rangle$ [37, 41]

Note that the light-cone (emanating from the space-time point $t = 0, x = x_+$) lies far ahead of the transmitted wavepacket. Indeed, although the wavepacket is ultrarelativistic ($p_0 = 100$ a.u.) the mean velocity, roughly estimated as $u \simeq pc/\sqrt{p^2 + m^2c^2} = 0.59c$ is still far from c . A computation of the momentum distribution of the initial state shows that coefficients $|g_+(p)|$ with $p > p_0 + 20$ a.u. become vanishingly small and do not contribute to the wavepacket, while any contribution with $p > 153.2$ a.u. would go over the barrier and would therefore not tunnel.

2. Case 2

Fig. 2 shows the situation for a higher barrier ($V_0 = 1.77mc^2$) at $t_p = 3 \times 10^{-3}$ a.u. Pair-production is still small, as the total number of electrons due to pair production is $N_{vac}(t_p)/2 = 0.31$ [see Eq. (20)], but the transmitted wavepacket amplitude is even smaller. As a result, the transmitted wavepacket appears as a small bump in the overall density (red line in Fig. 2). This is confirmed by applying Eq. (19) that allows for the computation of the part of the density due to the wavepacket (blue line in Fig. 2). Note that some of the works [17–25] investigating relativistic tunneling within the first quantized approximation have computed numerical results for barrier heights in cases in which QFT calculations show that the tiny amplitude of the transmitted wavepacket would be completely overshadowed by the larger (or much larger if supercritical barriers are considered) electron density produced by the barrier.

Fig. 2 also shows the light cone, emanating from the right edge x_+ of the initial wavepacket density distribution; it can be seen that although the electron is in the relativistic regime (the mean velocity of the initial distribution is $0.83c$), the transmitted wavepacket remains well inside the light cone, in line with the results of Sec. III.

C. Klein tunneling

Klein tunneling takes place for supercritical potentials ($V_0 > 2mc^2$) and wavepacket energies for which $(E - V_0)^2 > m^2c^4$; in this case the transmission of the electron wavepacket is mediated by pair production [31, 43] giving rise to an oscillating density inside the barrier. These modulations in pair-production give rise to a transmitted wavepacket with an

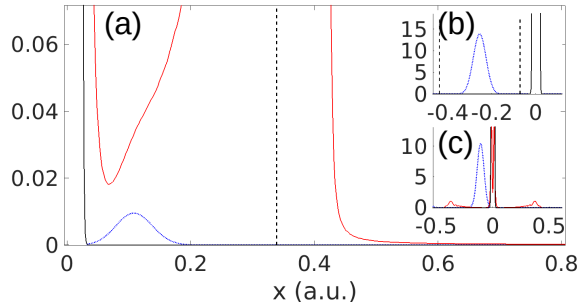


Figure 2. Numerical computations corresponding to Case 2, i.e. standard tunneling with a slightly radiating potential $V_0 = 1.77mc^2$. (a) The *total* density of the transmitted wavepacket is shown in red. The transmitted wavepacket is barely visible as a bump in the total density, although calculations show the wavepacket density (dotted blue). The inset displays snapshots of the wavepacket dynamics at (b) $t = 0$ and at (c) $t = 3 \times 10^{-3}$ (the time of the plot (a)). The initial wavepacket parameters are (in a.u.) $x_0 = -35\lambda$, $p_0 = 200$ and $\mathcal{D} = 16\lambda$ and for the barrier $L = 4\lambda$ and $\varepsilon = 0.3\lambda$, where $\lambda = \hbar/mc$.

undamped amplitude (as opposed to an exponentially decreasing transmission in the case of regular tunneling). Relative to the freely propagated wavepacket, the transmitted Klein tunneled one can be accelerated by the barrier (since the negative energy wavepacket components see a potential well [44]) but never faster than light, since our result Eq. (30) holds for any type of potential barrier. A computation illustrating Klein tunneling is given in Fig. 3, for $V_0 = 9mc^2$.

V. DISCUSSION AND CONCLUSION

Although we have shown in Sec. III that according to our space-time resolved relativistic QFT framework to spin-1/2 fermions there can be no superluminality in tunneling transmission, it is often asserted that tunneling can be superluminal or instantantaneous. It is worthwhile briefly recalling on which grounds such assertions have been made.

First, we must discard models based on non-relativistic frameworks, like the Schrödinger equation, for which propagation is indeed instantaneous [45]. The same holds for semi-classical approaches based on the Schrödinger equation. Experimental results, in particular those involving the attoclock technique in strong field ionization (see e.g. [2, 5, 10, 11]), have

usually relied on such models when estimating tunneling times. Superluminality appears here as an artifact of employing a non-relativistic approach.

Second, there is the problem of defining traversal times during the tunneling process. Indeed, there is no unambiguous manner to define a tunneling time [15]. Various candidates have been proposed (phase delays, dwell times, Larmor times, time operators, weak values). These quantities not only lead to conflicting results (predicting strikingly different traversal times) but furthermore by construction they can yield superluminal values, including when they are employed with relativistic wave equations [17, 19–21, 23, 25].

Third, some first quantized works based on relativistic wave equations have suggested superluminal transmission based on the fact that the maximum of the density (or of the current density) of the transmitted wavepacket arrives earlier than the maximum of the freely propagating one [18, 23, 24]. We note that in the three numerical cases given in Sec. IV we can also observe the same phenomenon: as illustrated in Fig. 4 the maximum of the tunneled wavepacket has traveled, at a given time, a longer distance than the maximum of an initially identical wavepacket that would have evolved freely. This is of course compatible with the

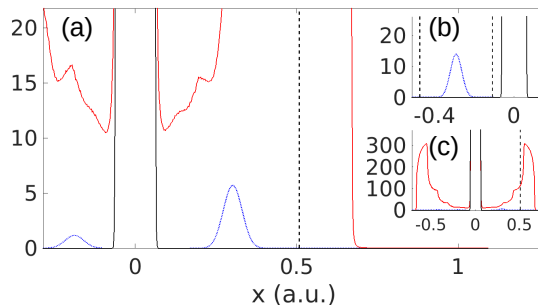


Figure 3. Numerical results for Case 3 (Klein tunneling), with a supercritical barrier of height $V_0 = 9mc^2$. (a) The electron wavepacket density is shown (dotted blue) at $t = 4.5 \times 10^{-3}$ a.u. well after the transmitted wavepacket (centered at $x \approx 0.3$ a.u.) has exited the barrier (solid vertical lines). Note that the transmitted wavepacket density is significantly larger than the one of the reflected wavepacket (centered at $x = -0.19$ a.u. and moving toward the left). (b) The initial wavepacket (light blue) is shown along with the support \mathcal{D} (dashed lines) and the barrier. (c) The plot (a) is zoomed out in order to visualize the electron density due to pair production (red line). The wavepacket is not visible at this scale. The initial wavepacket parameters in a.u. are $x_0 = -40\lambda, p_0 = 450$ a.u. and $\mathcal{D} = 16\lambda$ and for the barrier $L = 16\lambda$ and $\varepsilon = 0.3\lambda$ with $\lambda = \hbar/mc$.

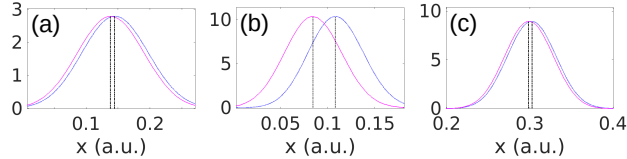


Figure 4. (a), (b) and (c) display for each case considered respectively in Figs. 1, 2 and 3, the position of the transmitted peak along with the position of the same initial wavepacket that would have evolved freely. The vertical dotted lines indicate the maxima of the transmitted peak and the free wavepackets (see text for details).

causal dynamics implied by Eq. (30). Indeed, having the maximum of a peak appearing earlier at a given position does not imply faster or superluminal dynamics: the important point is that the “advanced” peak still lies within the envelope of the free wavepacket.

Note that even within first quantized quantum mechanics it would be incorrect to associate part of the quantum state (the transmitted wavepacket) with a single particle somehow emerging faster from the barrier. Such a view would be clearly incompatible with a QFT based framework. According to QFT, a particle at each space-time point of a wavepacket is seen as a field excitation at that particular point, and the field excitation at that point can only be related causally to the field excitation at some other space-time point, in particular to the field excitation at a different position in a given reference frame. Put differently, the causality implied by Eq. (30) only imposes that the field excitation at the maximum of the transmitted wavepacket must lie within the forward light-cone emanating from \mathcal{D} .

To sum up, we have investigated the tunneling wavepacket dynamics for an electron within a relativistic QFT framework in which the barrier is modeled as a background field. We have shown that if the electron wavepacket is initially ($t = 0$) localized to the left of the barrier, the electron density at a space-like separated point to the right of the barrier does not depend on the presence or absence of the wavepacket at $t = 0$, thereby precluding any superluminal effects related to tunneling. We have numerically computed the space-time resolved electron density in typical cases of tunneling with potentials below, close to or above the supercritical value. We hope our results will contribute in clarifying the models and approximations employed when accounting for results involving traversal or detection times in tunneling related effects. We can expect similar results to hold for other types of relativistic quantum fields known to obey microcausality.

Acknowledgments. We are grateful for grant PID2021-126273NB-I00, funded by MCIN/AEI/10.13039/501100011033 and “ERDF A way of making Europe”. We acknowledge financial support from the Basque Government, grant No. IT1470-22. MP acknowledges support from the Spanish Agencia Estatal de Investigacion, grant No. PID2022-141283NB-100.

Appendix A: Field operators: equal-time anti-commutators

We prove here the equal-time anti-comutator given by Eq. (12) with the field operator $\hat{\Phi}(t, x)$ given in terms of the annihilation operators of particles and antiparticles by Eq. (10).

1. Field free case

In the *field free* case, the time evolution of the creation and annihilation operators is trivial ($\hat{b}_p(t) = e^{iE_p t} \hat{b}_p$, $\hat{d}_p^\dagger(t) = e^{-iE_p t} \hat{d}_p^\dagger$, etc.) and the equal-time anti-commutator reads

$$\begin{aligned} & [\hat{\Phi}^\dagger(x), \hat{\Phi}(y)]_+ = \\ & \left[\int dp \hat{b}_p^\dagger v_p^\dagger(x) e^{iE_p t} + \int dp \hat{d}_p^\dagger w_p^\dagger(x) e^{-iE_p t}, \int dp' \hat{b}_{p'} v_{p'}(y) e^{-iE_{p'} t} + \int dp' \hat{d}_{p'} w_{p'}(y) e^{-iE_{p'} t} \right]_+ \end{aligned} \quad (\text{A1})$$

Using the anti-commutation relations

$$\begin{aligned} & [\hat{b}_p^\dagger, \hat{b}_{p'}]_+ = [\hat{d}_p^\dagger, \hat{d}_{p'}]_+ = \delta(p - p'), \\ & [\hat{b}_p^\dagger, \hat{d}_{p'}]_+ = [\hat{d}_p^\dagger, \hat{b}_{p'}]_+ = \delta(p - p'), \end{aligned} \quad (\text{A2})$$

and

$$\begin{aligned} & v_p^\dagger(x) v_p(y) = e^{ip(y-x)} \\ & w_p^\dagger(x) w_p(y) = e^{-ip(x-y)}, \end{aligned} \quad (\text{A3})$$

we obtain

$$[\hat{\Phi}^\dagger(x), \hat{\Phi}(y)]_+ = \int dp (e^{ip(y-x)} + e^{ip(x-y)}) \quad (\text{A4})$$

which leads to Eq. (12) of the paper.

2. Background potential

In the presence of a *background potential*, the equal-time anti-commutation relation

$$[\hat{\Phi}^\dagger(t, x), \hat{\Phi}(t, y)]_+ = \left[\int dp (\hat{b}_p^\dagger(t) v_p^\dagger(x) + \hat{d}_p^\dagger(t) w_p(x)^\dagger), \int dp (\hat{b}_p(t) v_p(x) + \hat{d}_p(t) w_p(x)) \right]_+ \quad (\text{A5})$$

involves the anti-commutators of the type

$$[\hat{b}_{p_1}^\dagger(t), b_{p_2}(t)] = \left[\int dp'_1 \left(U_{v_{p_1} w_{p'_1}}^* \hat{b}_{p'_1}^\dagger + U_{v_{p_1} w_{p'_1}}^* \hat{d}_{p'_1}^\dagger \right), \int dp'_2 \left(U_{v_{p_2} v_{p'_2}} \hat{b}_{p'_2} + U_{v_{p_2} w_{p'_2}} \hat{d}_{p'_2}^\dagger \right) \right]_+. \quad (\text{A6})$$

Using Eq. (5) of the main text, one obtains

$$\begin{aligned} & [\hat{b}_{p_1}^\dagger(t), b_{p_2}(t)]_+ \\ &= \int dp'_1 \left(U_{v_{p_1} v_{p'_1}}^* U_{v_{p_2} v_{p'_1}} + U_{v_{p_1} w_{p'_1}}^* U_{v_{p_2} w_{p'_1}} \right) \\ &= \int dp'_1 \left(\langle v_{p_2} | \hat{U} | v_{p'_1} \rangle \langle v_{p'_1} | \hat{U}^\dagger | v_{p_1} \rangle + \langle v_{p_2} | \hat{U} | w_{p'_1} \rangle \langle w_{p'_1} | \hat{U}^\dagger | v_{p_1} \rangle \right) \\ &= \langle v_{p_2} | \hat{U} \hat{U}^\dagger | v_{p_1} \rangle = \langle v_{p_2} | v_{p_1} \rangle = \delta(p_1 - p_2), \end{aligned} \quad (\text{A7})$$

where in the last line, we used the completeness relation:

$$\int dp' (|v_{p'}\rangle \langle v_{p'}| + |w_{p'}\rangle \langle w_{p'}|) = 1$$

and the orthonormality of the solutions of the free Dirac equation. Similarly, we find that

$$[\hat{d}_{p_1}^\dagger(t), d_{p_2}(t)]_+ = \delta(p_1 - p_2). \quad (\text{A8})$$

Plugging-in these anti-commutators into Eq. (A5) leads to

$$[\hat{\Phi}^\dagger(t, x), \hat{\Phi}(t, y)]_+ = \int dp (e^{ip(y-x)} + e^{ip(x-y)}) \quad (\text{A9})$$

and hence again to Eq. (12) of the paper.

Appendix B: Derivation of the density expressions

We derive here the expression of the particle density, given by Eq. () which becomes Eq. (18).

Let us first compute the expectation value of the operator written in Eq. (14), written as

$$\begin{aligned} \rho_1(t, x) = \langle\langle 0 \parallel \int dp (g_+^*(p) \hat{b}_p + g_-^*(p) \hat{d}_p) \{ \iint dp_1 dp_2 v_{p_1}^\dagger(x) v_{p_2}(x) \int dp' (U_{v_{p_1} v_{p'}}^*(t) \hat{b}_{p'}^\dagger + U_{v_{p_1} w_{p'}}^*(t) \hat{d}_{p'}) \\ \int dp' (U_{v_{p_2} v_{p'}}(t) \hat{b}_{p'} + U_{v_{p_2} w_{p'}}(t) \hat{d}_{p'}^\dagger) \} \int dp (g_+(p) \hat{b}_p^\dagger + g_-(p) \hat{d}_p^\dagger) \parallel 0 \rangle\rangle \end{aligned} \quad (\text{B1})$$

which expands to

$$\begin{aligned} \rho_1(t, x) = \langle\langle 0 \parallel \int \dots \int dq_1 dq_1' dq_2 dq_2' dp_1 dp_2 g_-^*(q_1) g_-(q_2) U_{v_{p_1} w_{q_1'}}^*(t) U_{v_{p_2} w_{q_2'}}(t) v_{p_1}^\dagger(x) \Phi_{p_2}(x) \hat{d}_{q_1} \hat{d}_{q_1'} \hat{d}_{q_2'}^\dagger \hat{d}_{q_2}^\dagger \parallel 0 \rangle\rangle \\ + \langle\langle 0 \parallel \int \dots \int dq_1 dq_1' dq_2 dq_2' dp_1 dp_2 g_+^*(q_1) g_+(q_2) U_{v_{p_1} w_{q_1'}}^*(t) U_{v_{p_2} w_{q_2'}}(t) v_{p_1}^\dagger(x) v_{p_2}(x) \hat{b}_{q_1} \hat{d}_{q_1'} \hat{d}_{q_2'}^\dagger \hat{b}_{q_2}^\dagger \parallel 0 \rangle\rangle \\ + \langle\langle 0 \parallel \int \dots \int dq_1 dq_1' dq_2 dq_2' dp_1 dp_2 g_+^*(q_1) g_+(q_2) U_{v_{p_1} v_{q_1'}}^*(t) U_{v_{p_2} v_{q_2'}}(t) v_{p_1}^\dagger(x) v_{p_2}(x) \hat{b}_{q_1} \hat{b}_{q_1'}^\dagger \hat{b}_{q_2'}^\dagger \hat{b}_{q_2}^\dagger \parallel 0 \rangle\rangle. \end{aligned} \quad (\text{B2})$$

Using the anti-commutation relations of creation and annihilation operators

$$\begin{aligned} \langle\langle 0 \parallel \hat{d}_{q_1} \hat{d}_{q_1'} \hat{d}_{q_2'}^\dagger \hat{d}_{q_2}^\dagger \parallel 0 \rangle\rangle &= \delta_{q_1' q_2'} \delta_{q_1 q_2} - \delta_{q_1 q_2'} \delta_{q_1' q_2} \\ \langle\langle 0 \parallel \hat{b}_{q_1} \hat{d}_{q_1'} \hat{d}_{q_2'}^\dagger \hat{b}_{q_2}^\dagger \parallel 0 \rangle\rangle &= \delta_{q_1 q_2} \delta_{q_1' q_2'} \\ \langle\langle 0 \parallel \hat{b}_{q_1} \hat{b}_{q_1'}^\dagger \hat{b}_{q_2'}^\dagger \hat{b}_{q_2}^\dagger \parallel 0 \rangle\rangle &= \delta_{q_1 q_2'} \delta_{q_2 q_2'}, \end{aligned} \quad (\text{B3})$$

we get

$$\begin{aligned} \rho_1(t, x) = \int dq |g_-(q)|^2 \int dq \left(\int U_{v_p w_q}(t) v_p(x) \right)^\dagger \left(\int U_{v_p w_q}(t) v_p(x) \right) \\ + \int dq |g_+(q)|^2 \int dq \left(\int U_{v_p w_q}(t) v_p(x) \right)^\dagger \left(\int U_{v_p w_q}(t) v_p(x) \right) \\ + \left(\int dp dq g_+(p) U_{v_p v_q}(t) v_p(x) \right)^\dagger \left(\int dp dq g_+(p) U_{v_p v_q}(t) v_p(x) \right) \\ - \left(\int dp dq g_-(p) U_{v_p w_q}(t) v_p(x) \right)^\dagger \left(\int dp dq g_-(p) U_{v_p w_q}(t) v_p(x) \right). \end{aligned} \quad (\text{B4})$$

Using the normalization of the initial QFT state yields

$$\begin{aligned} \rho_1(t, x) = \int dq \left(\int U_{v_p w_q}(t) v_p(x) \right)^\dagger \left(\int U_{v_p w_q}(t) v_p(x) \right) \\ + \left(\int dp dq g_+(p) U_{v_p v_q}(t) v_p(x) \right)^\dagger \left(\int dp dq g_+(p) U_{v_p v_q}(t) v_p(x) \right) \\ - \left(\int dp dq g_-(p) U_{v_p w_q}(t) v_p(x) \right)^\dagger \left(\int dp dq g_-(p) U_{v_p w_q}(t) v_p(x) \right). \end{aligned} \quad (\text{B5})$$

The first line in the expression of $\rho_1(t, x)$ represents the electron density created by the background potential due to the vacuum excitation while the second line represents the

density corresponding to the incoming particle. The third line represents the modulation in the number density of the created particles due to the incident particle wave packet. The terms $\rho_2(t, x)$ and $\rho_3(t, x)$ are computed similarly, yielding

$$\begin{aligned} \rho_2(t, x) = & \int dp \left(\int dq U_{w_p v_q}(t) w_p(x) \right)^\dagger \left(\int dq U_{w_p v_q}(t) w_p(x) \right) \\ & + \left(\int dp dq g_-(q) U_{w_p w_q}(t) w_p(x) \right)^\dagger \left(\int dp dq g_-(q) U_{w_p w_q}(t) w_p(x) \right) \\ & - \left(\int dp dq g_+(q) U_{w_q w_p}(t) w_p(x) \right)^\dagger \left(\int dp dq g_+(q) U_{w_q v_q}(t) w_p(x) \right) \end{aligned} \quad (\text{B6})$$

and

$$\begin{aligned} \rho_3(t, x) = & 2\Re \left(\int dp dq g_-^*(q) U_{w_p w_q}^*(t) g_+(q) U_{v_p v_q} w_q^\dagger(x) v_p(x) \right) \\ & + 2\Re \left(\int dp dq g_-^*(q) U_{w_p v_q}^*(t) g_+(q) U_{v_p w_q} w_q^\dagger(x) v_p(x) \right) \end{aligned} \quad (\text{B7})$$

$\rho_2(t, x)$ is the counterpart of $\rho_1(t, x)$ for the positron density while $\rho_3(t, x)$ involves cross terms between positive and negative energy modes of the initial wave-packet. $\rho_3(t, x)$ cancels the infinite tails of $\rho_1(t, x)$ and $\rho_2(t, x)$. When integrated over the entire space however the contribution of this term vanishes, ensuring that ρ obeys

$$\int dx \rho(t, x) = \int dx \rho_1(t, x) + \int dx \rho_2(t, x) \quad (\text{B8})$$

which is the sum of the particle and antiparticle numbers.

-
- [1] M. Garg and K. Kern, Attosecond coherent manipulation of electrons in tunneling microscopy, *Science* 367, 411 (2019).
 - [2] Sainadh, U.S., Xu, H., Wang, X. et al. Attosecond angular streaking and tunnelling time in atomic hydrogen. *Nature* 568, 75 (2019).
 - [3] David C. Spierings and Aephraim M. Steinberg, Observation of the Decrease of Larmor Tunneling Times with Lower Incident Energy, *Phys. Rev. Lett.* 127, 133001 (2021).
 - [4] Zhenning Guo, Yiqi Fang, Peipei Ge, Xiaoyang Yu, Jiguo Wang, Meng Han, Qihuang Gong, and Yunquan Liu, Probing tunneling dynamics of dissociative H₂ molecules using two-color bicircularly polarized fields, *Phys. Rev. A* 104, L051101 (2021).
 - [5] Yu, M., Liu, K., Li, M. et al., Full experimental determination of tunneling time with attosecond-scale streaking method, *Light Sci Appl* 11, 215 (2022).

- [6] Yoo Kyung Lee, Hanzhen Lin, and Wolfgang Ketterle, Spin Dynamics Dominated by Resonant Tunneling into Molecular States, *Phys. Rev. Lett.* 131, 213001 (2023).
- [7] Mirza M. Elahi, Hamed Vakili, Yihang Zeng, Cory R. Dean, and Avik W. Ghosh, Direct Evidence of Klein and Anti-Klein Tunneling of Graphitic Electrons in a Corbino Geometry, *Phys. Rev. Lett.* 132, 146302 (2024).
- [8] J. G. Muga and C. R. Leavens, Arrival time in quantum mechanics, *Phys. Rep.* 338, 353 (2000).
- [9] U Satya Sainadh, R T Sang and I V Litvinyuk, Attoclock and the quest for tunnelling time in strong-field physics, *J. Phys. Photonics* 2 042002 (2020).
- [10] P. Eckle, A. N. Pfeiffer, C. Cirelli, A. Staudte, R. Džeržić, H. G. Müller, M. B. J. van Meer, and U. Keller, *Science* 322, 1525 (2008).
- [11] Pfeiffer, A., Cirelli, C., Smolarski, M. et al. Attoclock reveals natural coordinates of the laser-induced tunnelling current flow in atoms. *Nature Phys* 8, 76–80 (2012).
- [12] Tomasz Zimmermann, Siddhartha Mishra, Brent R. Doran, Daniel F. Gordon, and Alexandra S. Landsman, Tunneling Time and Weak Measurement in Strong Field Ionization, *Phys. Rev. Lett.* 116, 233603 (2016).
- [13] Masahiro Hino, Norio Achiwa, Seiji Tasaki, Toru Ebisawa, Takeshi Kawai, Tsunekazu Akiyoshi, and Dai Yamazaki, *Phys. Rev. A* 59, 2261 (1999).
- [14] P. Février and J. Gabelli, Tunneling time probed by quantum shot noise, *Nat Commun* 9, 4940 (2018).
- [15] D. Sokolovski and E. Akhmatskaya, No time at the end of the tunnel. *Commun Phys* 1, 47 (2018).
- [16] M. Klaiber, Q. Z. Lv, S. Sukiasyan, D. Bakucz Canario, K. Z. Hatsagortsyan, and C. H. Keitel, Reconciling Conflicting Approaches for the Tunneling Time Delay in Strong Field Ionization, *Phys. Rev. Lett.* 129, 203201 (2022).
- [17] P. Krekora, Q. Su, and R. Grobe, Effects of relativity on the time-resolved tunneling of electron wave packets, *Phys. Rev. A* 63, 032107 (2001).
- [18] V. Petrillo and D. Janner, Relativistic analysis of a wave packet interacting with a quantum-mechanical barrier, *Phys. Rev. A* 67, 012110 (2003).
- [19] Herbert G. Winful, Moussa Ngom, and Natalia M. Litchinitser, Relation between quantum tunneling times for relativistic particles, *Phys. Rev. A* 70, 052112 (2004); Erratum *Phys. Rev. A* 108, 019902 (2023).

- [20] S. De Leo and P.P. Rotelli, Dirac equation studies in the tunneling energy zone, *Eur. Phys. J. C* 51, 241 (2007).
- [21] A. E. Bernardini, Delay time computation for relativistic tunneling particles, *Eur. Phys. J. C* 55, 125 (2008).
- [22] O. del Barco and V. Gasparian, Relativistic tunnelling time for electronic wave packets, *J. Phys. A: Math. Theor.* 44 015303 (2011).
- [23] S. De Leo, A study of transit times in Dirac tunneling, *J. Phys. A: Math. Theor.* 46 15530 (2013).
- [24] R. S. Dumont, T. Rivlin, and E. Pollak, The relativistic tunneling flight time may be superluminal, but it does not imply superluminal signaling, *New J. Phys.* 22, 093060 (2020).
- [25] P. C. Flores and E. A. Galapon, Instantaneous tunneling of relativistic massive spin-0 particles, *EPL* 141 10001 (2023).
- [26] J. C. Park and Y. J. Lee, Superluminality and Causality in the Relativistic Barrier Problem, *J. Korean Phys. Soc.* 43, 4 (2003).
- [27] C. Anastopoulos and N. Savvidou, Quantum temporal probabilities in tunneling systems, *Ann. Phys.* 336, 281 (2013).
- [28] M. Alkhateeb, X. Gutierrez de la Cal, M. Pons, D. Sokolovski and A. Matzkin, Relativistic time-dependent quantum dynamics across supercritical barriers for Klein-Gordon and Dirac particles, *Phys. Rev. A* 103, 042203 (2021).
- [29] L. Gavassino and M. M. Disconzi, Subluminality of relativistic quantum tunneling, *Phys. Rev. A* 107, 032209 (2023).
- [30] T. Cheng, Q. Su, and R. Grobe, Introductory review on quantum field theory with space-time resolution, *Contemp. Phys.* 51, 315 (2010).
- [31] M. Alkhateeb and A. Matzkin, Space-time-resolved quantum field approach to Klein-tunneling dynamics across a finite barrier, *Phys. Rev. A* 106, L060202 (2022).
- [32] J. Unger, S. Dong, Q. Su, and R. Grobe, Optimal supercritical potentials for the electron-positron pair-creation rate, *Phys. Rev. A* 100, 012518 (2019).
- [33] D.D. Su, Y.T. Li, Q.Z. Lv, and J. Zhang, Enhancement of pair creation due to locality in bound-continuum interactions, *Phys. Rev. D* 101, 054501 (2020).
- [34] S. P. Gavrilov and D. M. Gitman, Consistency Restrictions on Maximal Electric-Field Strength in Quantum Field Theory, *Phys. Rev. Lett.* 101, 130403 (2008).

- [35] H. Feshbach and F. Villars, Elementary Relativistic Wave Mechanics of Spin 0 and Spin 1/2 Particles, *Rev. Mod. Phys.* 30, 24 (1958).
- [36] Stephen A. Fulling, *Aspects of Quantum Field Theory in Curved Spacetime* (Cambridge Univ. Press, Cambridge, Great Britain, 1989).
- [37] M. Alkhateeb and A. Matzkin, Evolution of strictly localized states in noninteracting quantum field theories with background fields, *Phys. Rev. A* 109, 062223 (2024).
- [38] W. Greiner, *Field Quantization* (Springer-Verlag, Berlin, 1996).
- [39] C. J. Fewster and K. Rejzner, Algebraic Quantum Field Theory ? an introduction, in F. Finster et al. (Eds), *Progress and Visions in Quantum Theory in View of Gravity* (Springer, 2020) [arXiv:1904.04051]
- [40] Thanu Padmanabhan, *Quantum Field Theory* (Springer International Publishing Switzerland, 2016).
- [41] S. S. Schweber, *An Introduction to Relativistic Quantum Field Theory* (Dover, New York, 2005).
- [42] M. Ruf, H. Bauke and C. H. Keitel, *J. Comp. Phys.* 228 9092 (2009).
- [43] P. Krekora, Q. Su, and R. Grobe, Klein Paradox in Spatial and Temporal Resolution, *Phys. Rev. Lett.* 92, 040406 (2004).
- [44] N. Dombey and A. Calogeracos, Seventy years of the Klein paradox, *Phys. Rep.* 315, 41 (1999).
- [45] Gerhard C. Hegerfeldt and Simon N. M. Ruijsenaars, Remarks on causality, localization, and spreading of wave packets, *Phys. Rev. D* 22, 377 (1980).